Evidence for the Suppressed Decay $B^- \to DK^-$, $D \to K^+\pi^-$

Y. Horii,[47] K. Trabelsi,[8] H. Yamamoto,[47] I. Adachi,[8] H. Aihara,[48] K. Arinstein,[1,35] V. Aulchenko,[1,35] T. Aushev,[21,14] V. Balagura,[14] E. Barberio,[25] K. Belous,[13] B. Bhuyan,[10] M. Bischofberger,[27] A. Bozek,[31] M. Bračko,[23,15] T. E. Browder,[7] M. -C. Chang,[4] P. Chang,[30] A. Chen,[28] P. Chen,[30] B. G. Cheon,[6] C. -C. Chiang,[30] I. -S. Cho,[53] K. Cho,[18] Y. Choi,[42] Z. Doležal,[2] S. Eidelman,[1,35] M. Feindt,[17] V. Gaur,[44] N. Gabyshev,[1,35] A. Garmash,[1,35] B. Golob,[22,15] H. Ha,[19] J. Haba,[8] K. Hayasaka,[26] Y. Hoshi,[46] W. -S. Hou,[30] Y. B. Hsiung,[30] H. J. Hyun,[20] T. Iijima,[26] K. Inami,[26] A. Ishikawa,[39] R. Itoh,[8] M. Iwabuchi,[53] Y. Iwasaki,[8] T. Iwashita,[27] N. J. Joshi,[44] T. Julius,[25] J. H. Kang,[53] T. Kawasaki,[33] H. Kichimi,[8] C. Kiesling,[24] H. J. Kim,[20] H. O. Kim,[20] M. J. Kim,[20] Y. J. Kim,[18] K. Kinoshita,[3] B. R. Ko,[19] N. Kobayashi,[49] S. Korpar,[23,15] P. Križan,[22,15] T. Kuhr,[17] R. Kumar,[37] Y. -J. Kwon,[53] M. J. Lee,[41] S. -H. Lee,[19] J. Li,[7] C. Liu,[40] D. Liventsev,[14] R. Louvot,[21] A. Matyja,[31] S. McOnie,[43] K. Miyabayashi,[27] H. Miyata,[33] Y. Miyazaki,[26] G. B. Mohanty,[44] A. Moll,[24,45] T. Mori,[26] N. Muramatsu,[38] E. Nakano,[36] H. Nakazawa,[28] Z. Natkaniec,[31] S. Neubauer,[17] S. Nishida,[8] O. Nitoh,[51] T. Ohshima,[26] S. Okuno,[16] Y. Onuki,[47] P. Pakhlov,[14] G. Pakhlova,[14] C. W. Park,[42] H. K. Park,[20] R. Pestotnik,[15] M. Petrič,[15] L. E. Piilonen,[52] A. Poluektov,[1,35] M. Prim,[17] K. Prothmann,[24,45] M. Röhrken,[17] S. Ryu,[41] H. Sahoo,[7] Y. Sakai,[8] O. Schneider,[21] C. Schwanda,[12] A. J. Schwartz,[3] K. Senyo,[26] O. Seon,[26] M. E. Sevior,[25] M. Shapkin,[13] V. Shebalin,[1,35] C. P. Shen,[7] T. -A. Shibata,[49] J. -G. Shiu,[30] F. Simon,[24,45] P. Smerkol,[15] Y. -S. Sohn,[53] E. Solovieva,[14] S. Stanič,[34] M. Starič,[15] M. Sumihama,[5] T. Sumiyoshi,[50] S. Suzuki,[39] S. Tanaka,[8] Y. Teramoto,[36] M. Uchida,[49] S. Uehara,[8] T. Uglov,[14] Y. Unno,[6] S. Uno,[8] Y. Usov,[1,35] G. Varner,[7] A. Vinokurova,[1,35] A. Vossen,[9] C. H. Wang,[29] P. Wang,[11] M. Watanabe,[33] Y. Watanabe,[16] J. Wicht,[8] E. Won,[19] B. D. Yabsley,[43] Y. Yamashita,[32] D. Zander,[17] Z. P. Zhang,[40] V. Zhulanov,[1,35] and A. Zupanc[17]

(Belle Collaboration)

[1]*Budker Institute of Nuclear Physics, Novosibirsk*
[2]*Faculty of Mathematics and Physics, Charles University, Prague*
[3]*University of Cincinnati, Cincinnati, Ohio 45221*
[4]*Department of Physics, Fu Jen Catholic University, Taipei*
[5]*Gifu University, Gifu*
[6]*Hanyang University, Seoul*
[7]*University of Hawaii, Honolulu, Hawaii 96822*
[8]*High Energy Accelerator Research Organization (KEK), Tsukuba*
[9]*University of Illinois at Urbana-Champaign, Urbana, Illinois 61801*
[10]*Indian Institute of Technology Guwahati, Guwahati*
[11]*Institute of High Energy Physics, Chinese Academy of Sciences, Beijing*
[12]*Institute of High Energy Physics, Vienna*
[13]*Institute of High Energy Physics, Protvino*
[14]*Institute for Theoretical and Experimental Physics, Moscow*
[15]*J. Stefan Institute, Ljubljana*
[16]*Kanagawa University, Yokohama*
[17]*Institut für Experimentelle Kernphysik, Karlsruher Institut für Technologie, Karlsruhe*
[18]*Korea Institute of Science and Technology Information, Daejeon*
[19]*Korea University, Seoul*
[20]*Kyungpook National University, Taegu*
[21]*École Polytechnique Fédérale de Lausanne (EPFL), Lausanne*
[22]*Faculty of Mathematics and Physics, University of Ljubljana, Ljubljana*
[23]*University of Maribor, Maribor*
[24]*Max-Planck-Institut für Physik, München*
[25]*University of Melbourne, School of Physics, Victoria 3010*
[26]*Nagoya University, Nagoya*
[27]*Nara Women's University, Nara*
[28]*National Central University, Chung-li*
[29]*National United University, Miao Li*
[30]*Department of Physics, National Taiwan University, Taipei*
[31]*H. Niewodniczanski Institute of Nuclear Physics, Krakow*
[32]*Nippon Dental University, Niigata*
[33]*Niigata University, Niigata*

[34]University of Nova Gorica, Nova Gorica
[35]Novosibirsk State University, Novosibirsk
[36]Osaka City University, Osaka
[37]Panjab University, Chandigarh
[38]Research Center for Nuclear Physics, Osaka University, Osaka
[39]Saga University, Saga
[40]University of Science and Technology of China, Hefei
[41]Seoul National University, Seoul
[42]Sungkyunkwan University, Suwon
[43]School of Physics, University of Sydney, NSW 2006
[44]Tata Institute of Fundamental Research, Mumbai
[45]Excellence Cluster Universe, Technische Universität München, Garching
[46]Tohoku Gakuin University, Tagajo
[47]Tohoku University, Sendai
[48]Department of Physics, University of Tokyo, Tokyo
[49]Tokyo Institute of Technology, Tokyo
[50]Tokyo Metropolitan University, Tokyo
[51]Tokyo University of Agriculture and Technology, Tokyo
[52]CNP, Virginia Polytechnic Institute and State University, Blacksburg, Virginia 24061
[53]Yonsei University, Seoul

(Received 30 March 2011; published 10 June 2011)

The suppressed decay chain $B^- \to DK^-$, $D \to K^+\pi^-$, where D indicates a $\bar{D}^0$ or D^0 state, provides important information on the CP-violating angle ϕ_3. We measure the ratio $\mathcal{R}_{DK}$ of the decay rates to the favored mode $B^- \to DK^-$, $D \to K^-\pi^+$ to be $\mathcal{R}_{DK} = [1.63^{+0.44}_{-0.41}(\text{stat})^{+0.07}_{-0.13}(\text{syst})] \times 10^{-2}$, which indicates the first evidence of the signal with a significance of 4.1σ. We also measure the asymmetry $\mathcal{A}_{DK}$ between the charge-conjugate decays to be $\mathcal{A}_{DK} = -0.39^{+0.26}_{-0.28}(\text{stat})^{+0.04}_{-0.03}(\text{syst})$. The results are based on the full 772×10^6 $B\bar{B}$ pair data sample collected at the $\Upsilon(4S)$ resonance with the Belle detector.

DOI: 10.1103/PhysRevLett.106.231803 PACS numbers: 13.25.Hw, 11.30.Er, 12.15.Hh, 14.40.Nd

Determinations of the parameters of the standard model are fundamentally important; any significant discrepancy between the expected and measured values would be a signature of new physics. The Cabibbo-Kobayashi-Maskawa matrix [1,2] consists of weak interaction parameters for the quark sector, one of which is the CP-violating angle $\phi_3 \equiv \arg(-V_{ud}V_{ub}^*/V_{cd}V_{cb}^*)$ [3]. Several methods proposed for measuring ϕ_3 exploit interference in the decay $B^- \to DK^-$ ($D = \bar{D}^0$ or D^0), where the two D states decay to a common final state [4–7]. One of the methods utilizes the decay $B^- \to DK^-$, $D \to K^+\pi^-$ [6]. The magnitudes of interfering amplitudes are comparable and hence can enhance the effects of CP violation. Previous studies of this decay mode have not found a significant signal yield [8,9].

In this analysis, we measure the ratio $\mathcal{R}_{DK}$ of the aforementioned suppressed decay to the favored decay, $B^- \to DK^-$, $D \to K^-\pi^+$, and the CP asymmetry $\mathcal{A}_{DK}$ defined as

$$\mathcal{R}_{DK} \equiv \frac{\mathcal{B}([K^+\pi^-]_D K^-) + \mathcal{B}([K^-\pi^+]_D K^+)}{\mathcal{B}([K^-\pi^+]_D K^-) + \mathcal{B}([K^+\pi^-]_D K^+)}, \quad (1)$$

$$\mathcal{A}_{DK} \equiv \frac{\mathcal{B}([K^+\pi^-]_D K^-) - \mathcal{B}([K^-\pi^+]_D K^+)}{\mathcal{B}([K^+\pi^-]_D K^-) + \mathcal{B}([K^-\pi^+]_D K^+)}, \quad (2)$$

where $[f]_D$ indicates the final state f originating from a $\bar{D}^0$ or D^0 meson. The same selection criteria and fitting functions are used for the suppressed decays and the favored decays wherever possible in order to cancel systematic uncertainties. The observables are related to ϕ_3 as follows:

$$\mathcal{R}_{DK} = r_B^2 + r_D^2 + 2r_B r_D \cos(\delta_B + \delta_D)\cos\phi_3, \quad (3)$$

$$\mathcal{A}_{DK} = 2r_B r_D \sin(\delta_B + \delta_D)\sin\phi_3/\mathcal{R}_{DK}, \quad (4)$$

where $r_B = |A(B^- \to \bar{D}^0 K^-)/A(B^- \to D^0 K^-)|$, $r_D = |A(D^0 \to K^+\pi^-)/A(\bar{D}^0 \to K^+\pi^-)|$, and δ_B (δ_D) is the strong phase difference between the two B (D) decay amplitudes appearing in the ratios. By combining other experimental inputs [10–12], the value of ϕ_3 can be extracted in a model-independent manner [5,6]. The decay $B^- \to D\pi^-$, $D \to K^+\pi^-$ is also analyzed as a reference. For this final state the decay rate is relatively large whereas the effect of ϕ_3 is small.

The results are based on the full 772×10^6 $B\bar{B}$ pair data sample collected at the $\Upsilon(4S)$ resonance with the Belle detector located at the KEKB asymmetric-energy e^+e^- collider [13]. The Belle detector is described in detail elsewhere [14]. The primary detector components used in this analysis are a tracking system consisting of a silicon vertex detector and a 50-layer central drift chamber (CDC), an array of aerogel threshold Cherenkov counters (ACC), and a barrel-like arrangement of time-of-flight scintillation counters (TOF).

Neutral D meson candidates are reconstructed from pairs of oppositely charged tracks. For each track, we apply a particle identification requirement based on information from the ACC and TOF, and specific ionization measurements from the CDC. The efficiency to identify a kaon or a pion is 85–95%, while the probability of misidentifying a pion (kaon) as a kaon (pion) is 10–20%. The invariant mass of the $K\pi$ pair is required to satisfy $1.850\ \mathrm{GeV}/c^2 < M(K\pi) < 1.880\ \mathrm{GeV}/c^2$, which corresponds to approximately $\pm 3\sigma$ around the world-average value of the D mass [15], where σ denotes the resolution in $M(K\pi)$. To improve the momentum determination, tracks from the D candidate are refitted with their invariant mass constrained to the nominal D mass.

B meson candidates are reconstructed by combining a D candidate with a charged hadron candidate. The signal is identified using the beam-energy-constrained mass (M_{bc}) and the energy difference (ΔE) defined, in the e^+e^- center-of-mass frame, as $M_{\mathrm{bc}} = \sqrt{E^2_{\mathrm{beam}} - |\vec{p}_B|^2}$ and $\Delta E = E_B - E_{\mathrm{beam}}$, where E_{beam} is the beam energy and $\vec{p}_B$ and E_B are the momentum and energy, respectively, of the B meson candidate. We require $5.271\ \mathrm{GeV}/c^2 < M_{\mathrm{bc}} < 5.287\ \mathrm{GeV}/c^2$, which corresponds to $\pm 3\sigma$ around the B mass value [15] with σ denoting the resolution in M_{bc}.

The dominant backgrounds arise from the continuum processes $e^+e^- \to q\bar{q}$ ($q = u, d, s, c$). In order to remove $D^{*\pm} \to D\pi^{\pm}$ decays produced in such a process, we employ the variable ΔM defined as the mass difference between the $D^{*\pm}$ and D candidates, where the $D^{*\pm}$ candidate is reconstructed from the D candidate used in the B reconstruction and a $\pi^{\pm}$ candidate not used in the B reconstruction. We require $\Delta M > 0.15\ \mathrm{GeV}/c^2$, which removes 28% of the $c\bar{c}$ background as well as some of the $B\bar{B}$ background. The loss of signal efficiency is 1.4%.

The $q\bar{q}$ background is further discriminated with a neural network technique based on the NEUROBAYES package [16]. The inputs to the network are (i) a Fisher discriminant [17] formed from modified Fox-Wolfram moments [18], (ii) the vertex separation between the B candidate and the remaining tracks, (iii) the cosine of the decay angle of $D \to K^+\pi^-$, where the decay angle is defined as the angle between the K^+ candidate and the B^- candidate in the rest frame of the D, (iv) the cosine of the angle between the B candidate and the beam axis in the e^+e^- center-of-mass frame, (v) the expected B flavor dilution factor that ranges from zero for no flavor information to unity for unambiguous flavor assignment [19], (vi) the cosine of the angle between the thrust axis of the B candidate and that of the rest of the event, where the thrust axis is oriented in such a way that the sum of momentum projections is maximized, and four other variables that exploit the kinematics of the events. The neural network is trained with Monte Carlo (MC) events. A requirement is applied on the network output (NB) that preserves 96% of the signal while rejecting 74% of the background.

There are a few background modes that can peak in the signal window (''peaking background''). The decay $B^- \to [K^+K^-]_D\pi^-$ may contribute to the background for $B^- \to [K^+\pi^-]_D K^-$ if the D candidate is misreconstructed. To reject this background, we veto candidates satisfying $1.840\ \mathrm{GeV}/c^2 < M(KK) < 1.890\ \mathrm{GeV}/c^2$. The favored decay $B^- \to [K^-\pi^+]_D h^-$ ($h = K$ or π) can also produce a peaking background for the suppressed decay if both the kaon and the pion from the D decay are misidentified and the particle assignments are interchanged. We thus veto candidates for which the invariant mass of the $K\pi$ pair is inside a $(1.865 \pm 0.020)\ \mathrm{GeV}/c^2$ window when the mass assignments are exchanged.

The signal yield is extracted from the two-dimensional distribution of ΔE and NB using an extended unbinned maximum likelihood fit. The fit is simultaneously applied to DK^-, DK^+, $D\pi^-$ and $D\pi^+$. The components of the fit are divided into signal, ''feed-across'', $B\bar{B}$ background, and $q\bar{q}$ background, as described in detail below. For each component, the correlation between ΔE and NB is found to be small. We thus obtain the probability density function (PDF) by taking a product of individual PDFs for ΔE and NB. For NB, we use one-dimensional histogram PDFs for all components.

For the ΔE signal PDF, we use a sum of two Gaussians whose parameters are fixed from the data for the favored modes. For NB, we obtain the PDF by applying $|\Delta E| < 0.01$ GeV to the same samples.

The $D\pi$ (DK) feed-across is the background from misidentified $D\pi$ (DK) final states that peaks in the fit to the DK ($D\pi$) sample. The shift due to the incorrect mass assignment makes the ΔE distribution asymmetric, and thus we use a sum of two asymmetric Gaussians, for which the left and right sides have different widths. The corresponding parameters for the $D\pi$ feed-across are obtained from the favored mode in data, while those for the DK feed-across are obtained from MC sample because of low statistics in the data. The PDFs for NB are obtained from the same reference samples used for ΔE calibration after applying the additional requirement $|\Delta E - 0.05\ \mathrm{GeV}| < 0.01$ GeV to the data sample. The K/π misidentification probabilities are fixed from the samples of the favored modes.

The $B\bar{B}$ background populates the entire ΔE region. This background is fitted with an exponential PDF that models the tails of the backgrounds from the modes $B^- \to D^*\pi^-$, $B^- \to D\rho^-$, and $B^- \to D^*K^-$, which peak in the negative ΔE region, as well as combinatorial backgrounds. The NB PDF is obtained from $B\bar{B}$ MC samples, in which all known B and $\bar{B}$ meson decays are included. The charge asymmetry for the $B\bar{B}$ background is floated in the fit.

The $q\bar{q}$ background distribution in ΔE is modeled by a linear function. The PDF of NB is obtained from a sideband sample of data: $5.20\ \mathrm{GeV}/c^2 < M_{\mathrm{bc}} < 5.26\ \mathrm{GeV}/c^2$ and $0.15\ \mathrm{GeV} < \Delta E < 0.30\ \mathrm{GeV}$. The charge asymmetry for the $q\bar{q}$ background is fixed to zero.

The results of the fits of the above PDFs to the final data samples are shown in Fig. 1. The signal yields and the reconstruction efficiencies are listed in Table I. Note that the rare charmless $b \to s$ decay $B^- \to K^+K^-\pi^-$ can peak inside the signal region for $B^- \to [K^+\pi^-]_D K^-$ and be included in the signal yield. To estimate its contribution as well as contributions from $B^- \to [K^+K^-]_D\pi^-$ and $B^- \to [K^-\pi^+]_D K^-$, we fit the $M(K\pi)$ data sidebands: $1.815\ \mathrm{GeV}/c^2 < M(K\pi) < 1.845\ \mathrm{GeV}/c^2$ and $1.885\ \mathrm{GeV}/c^2 < M(K\pi) < 2.005\ \mathrm{GeV}/c^2$. The sidebands are chosen to avoid the contribution from $B^- \to [K^+K^-]_D\pi^-$ caused by K/π misidentification. We apply the same fitting method used in the signal extraction to the sideband sample to obtain an expected yield of $-1.9^{+3.7}_{-3.5}$ events. For $B^- \to [K^+\pi^-]_D\pi^-$, we also apply the requirement $M(K\pi) < 1.915\ \mathrm{GeV}/c^2$ for the sideband sample to avoid $B^- \to [\pi^+\pi^-]_D\pi^-$ background, and obtain $-3.2^{+7.0}_{-6.4}$. We do not subtract these backgrounds from the signal yields but instead include the errors on the yields in the systematic uncertainties.

From the signal yields in Table I, we obtain

$$\mathcal{R}_{DK} = [1.63^{+0.44}_{-0.41}(\mathrm{stat})^{+0.07}_{-0.13}(\mathrm{syst})] \times 10^{-2}, \quad (5)$$

$$\mathcal{R}_{D\pi} = [3.28^{+0.38}_{-0.36}(\mathrm{stat})^{+0.12}_{-0.18}(\mathrm{syst})] \times 10^{-3}, \quad (6)$$

where the contributions to the systematic uncertainties are listed in Table II. The uncertainties due to the ΔE PDFs for the DK signal, the $D\pi$ signal, and the $D\pi$ feed-across are evaluated by varying the shape parameters by $\pm 1\sigma$. Those due to the DK feed-across are obtained by varying the width and the mean by $\pm 10\%$, which is the difference observed between the data and MC samples for the $D\pi$ feed-across. The uncertainties from the NB PDFs for the DK and $D\pi$ signals (the $D\pi$ feed-across) are estimated by obtaining PDFs from the region $0.01\ \mathrm{GeV} < |\Delta E| < 0.02\ \mathrm{GeV}$ $(0.01\ \mathrm{GeV} < |\Delta E - 0.05\ \mathrm{GeV}| < 0.02\ \mathrm{GeV})$. Those due to the DK feed-across and the $B\bar{B}$ background are estimated by using the DK signal PDF. Those due to the $q\bar{q}$ background are estimated by using $(M_{\mathrm{bc}}, \Delta E)$ different sidebands. The uncertainties due to the K/π misidentification probabilities for the feed-across backgrounds are obtained by varying their values by their $\pm 1\sigma$ errors. The uncertainty due to the charge asymmetry of the $q\bar{q}$ background is obtained by varying it by ± 0.02 (± 0.005) for DK ($D\pi$), which is the uncertainty in the favored DK ($D\pi$) signal. A possible fit bias is checked by generating 10 000 pseudoexperiments. The uncertainties in detection efficiencies mainly arise from MC statistics and the uncertainties in the particle identification efficiencies. The total systematic uncertainty is calculated by summing the above uncertainties in quadrature.

The significances of $\mathcal{R}_{DK}$ and $\mathcal{R}_{D\pi}$ are estimated using the fit likelihoods by convolving asymmetric Gaussians denoting the systematic uncertainties [8], and listed in Table I. The significance for $\mathcal{R}_{DK}$ is 4.1σ, which constitutes the first evidence for the suppressed DK decay.

The ΔE projections are shown separately for each charge of the B candidate in Fig. 2. We obtain

$$\mathcal{A}_{DK} = -0.39^{+0.26}_{-0.28}(\mathrm{stat})^{+0.04}_{-0.03}(\mathrm{syst}), \quad (7)$$

$$\mathcal{A}_{D\pi} = -0.04 \pm 0.11(\mathrm{stat})^{+0.02}_{-0.01}(\mathrm{syst}), \quad (8)$$

where the systematic uncertainties are evaluated in a similar manner as that done for $\mathcal{R}_{DK}$ and $\mathcal{R}_{D\pi}$ (see Table II). The uncertainty due to the yield of the peaking backgrounds is obtained by varying the signal yield in the denominator of the CP asymmetry. The uncertainty due to the asymmetry of the peaking backgrounds is negligible [20]. To account for possible bias due to the charge asymmetry of the detector, we take the uncertainty in the asymmetry of the favored signal as a conservative limit on this effect.

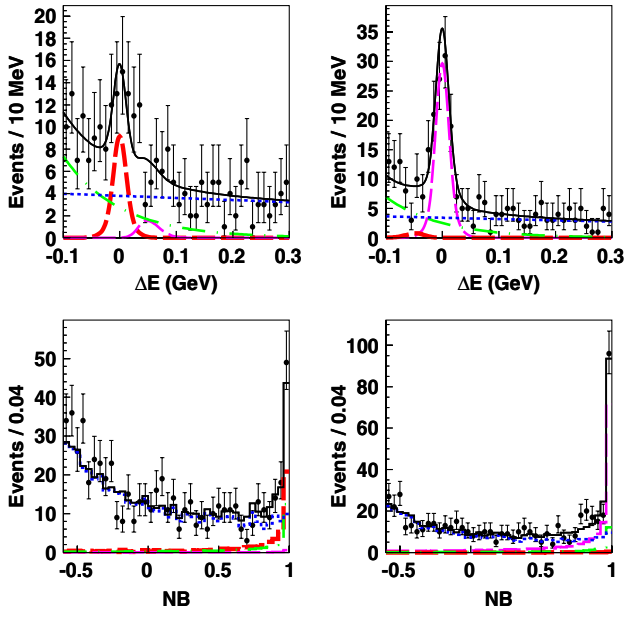

FIG. 1 (color online). ΔE $(NB > 0.9)$ and NB $(|\Delta E| < 0.03\ \mathrm{GeV})$ distributions for $[K^+\pi^-]_D K^-$ (left) and $[K^+\pi^-]_D\pi^-$ (right). Charge-conjugate decays are included. In these plots, $[K^+\pi^-]_D K^-$ components are shown by thicker dashed curves (red), and $[K^+\pi^-]_D\pi^-$ components are shown by thinner dashed curves (magenta). $B\bar{B}$ backgrounds are shown by dash-dotted curves (green) while $q\bar{q}$ backgrounds are shown by dotted curves (blue). The sums of all components are shown by solid curves (black).

TABLE I. Signal yields, reconstruction efficiencies and significances. Charge-conjugate modes are included. The uncertainties shown are statistical only.

Mode	Yield	Efficiency (%)	Significance
$B^- \to [K^+\pi^-]_D K^-$	$56.0^{+15.1}_{-14.2}$	33.6 ± 0.4	4.1σ
$B^- \to [K^-\pi^+]_D K^-$	3394^{+68}_{-69}	33.2 ± 0.4	
$B^- \to [K^+\pi^-]_D\pi^-$	$165.0^{+19.1}_{-18.1}$	36.5 ± 0.4	9.2σ
$B^- \to [K^-\pi^+]_D\pi^-$	49164^{+245}_{-244}	35.7 ± 0.4	

TABLE II. Summary of the systematic uncertainties. We use the notation "..." to denote negligible contributions.

Source	$\mathcal{R}_{DK}$	$\mathcal{R}_{D\pi}$	$\mathcal{A}_{DK}$	$\mathcal{A}_{D\pi}$
PDFs of ΔE	+2.1–1.8%	+1.3–1.2%	±0.01	±0.00
PDFs of NB	+3.4–3.0%	±3.1%	+0.02–0.01	±0.01
K/π misidentification	±0.2%	±0.0%	±0.00	±0.00
Asymmetry of $q\bar{q}$ background	+0.8–0.9%	±0.1%	±0.01	±0.00
Fit bias	−1.1%	−0.5%	−0.01	−0.00
Peaking backgrounds	−6.6%	−4.2%	+0.03	+0.00
Efficiency	±1.7%	±1.5%	...	...
Detector asymmetry	...	...	±0.02	±0.00
Total	+4.4–7.8%	+3.7–5.6%	+0.04–0.03	+0.02–0.01

Assuming Eqs. (3) and (4) and $r_B = 0.1$ [15], the values of $\mathcal{R}_{DK}$ and A_{DK} are restricted to the ranges $[0.2, 2.5] \times 10^{-2}$ and $[-0.9, 0.9]$, respectively, depending on the values of ϕ_3, δ_B, and δ_D. Our results are consistent with these expectations. The small experimental uncertainties in $\mathcal{R}_{DK}$ and A_{DK} thus provide important additional information on ϕ_3. The experimental results for $\mathcal{R}_{D\pi}$ and $A_{D\pi}$ are also consistent with the standard model [15].

In summary, we report measurements of the suppressed decay $B^- \to [K^+\pi^-]_D h^-$ ($h = K, \pi$) using the full 772×10^6 $B\bar{B}$ pair data sample collected with the Belle detector. We use a neural network-based method [16] to discriminate $q\bar{q}$ background from signal, impose a $D^{*\pm}$ veto, and employ a two-dimensional fit to extract the signal. These steps, along with a 20% increase in the data sample, result in a significant improvement compared to the previous analysis [8]. We obtain the first evidence for a DK signal with a significance of 4.1σ, and report the most precise measurements to date of the CP asymmetries and ratios of the suppressed decay rate to the favored decay rate. Our results will provide important ingredients in a model-independent extraction of ϕ_3 [5,6].

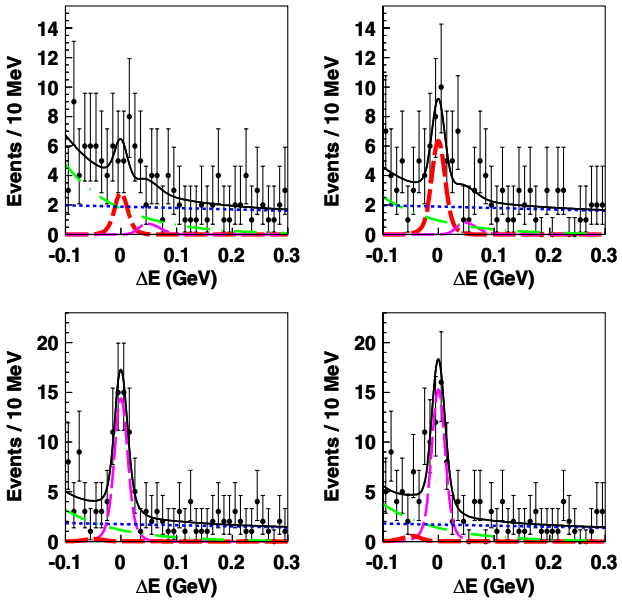

FIG. 2 (color online). ΔE distributions ($NB > 0.9$) for $[K^+\pi^-]_D K^-$ (left upper), $[K^-\pi^+]_D K^+$ (right upper), $[K^+\pi^-]_D \pi^-$ (left lower), and $[K^-\pi^+]_D \pi^+$ (right lower). The curves show the same components as in Fig. 1.

We thank the KEKB group for excellent operation of the accelerator, the KEK cryogenics group for efficient solenoid operations, and the KEK computer group and the NII for valuable computing and SINET3 network support. We acknowledge support from MEXT, JSPS and Nagoya's TLPRC (Japan); ARC and DIISR (Australia); NSFC (China); MSMT (Czechia); DST (India); MEST, NRF, NSDC of KISTI, and WCU (Korea); MNiSW (Poland); MES and RFAAE (Russia); ARRS (Slovenia); SNSF (Switzerland); NSC and MOE (Taiwan); and DOE (USA).

[1] N. Cabibbo, Phys. Rev. Lett. **10**, 531 (1963).
[2] M. Kobayashi and T. Maskawa, Prog. Theor. Phys. **49**, 652 (1973).
[3] This angle is also known as γ.
[4] I. I. Bigi and A. I. Sanda, Phys. Lett. B **211**, 213 (1988).
[5] M. Gronau and D. London, Phys. Lett. B **253**, 483 (1991); M. Gronau and D. Wyler, Phys. Lett. B **265**, 172 (1991).
[6] D. Atwood, I. Dunietz, and A. Soni, Phys. Rev. Lett. **78**, 3257 (1997); Phys. Rev. D **63**, 036005 (2001).
[7] A. Giri, Yu. Grossman, A. Soffer, and J. Zupan, Phys. Rev. D **68**, 054018 (2003); A. Bondar, *Proceedings of BINP Special Analysis Meeting on Dalitz Analysis, 2002* (unpublished).
[8] Y. Horii *et al.* (Belle Collaboration), Phys. Rev. D **78**, 071901(R) (2008).
[9] P. del Amo Sanchez *et al.* (BaBar Collaboration), Phys. Rev. D **82**, 072006 (2010).
[10] K. Abe *et al.* (Belle Collaboration), Phys. Rev. D **73**, 051106(R) (2006).
[11] P. del Amo Sanchez *et al.* (BaBar Collaboration), Phys. Rev. D **82**, 072004 (2010).
[12] D. Asner *et al.* (Heavy Flavor Averaging Group), arXiv:1010.1589, and online update for Charm at http://www.slac.stanford.edu/xorg/hfag/charm.
[13] S. Kurokawa and E. Kikutani, Nucl. Instrum. Methods Phys. Res., Sect. A **499**, 1 (2003), and other papers included in this volume.

[14] A. Abashian *et al.* (Belle Collaboration), Nucl. Instrum. Methods Phys. Res., Sect. A **479**, 117 (2002).
[15] K. Nakamura *et al.* (Particle Data Group), J. Phys. G **37**, 075021 (2010).
[16] M. Feindt and U. Kerzel, Nucl. Instrum. Methods Phys. Res., Sect. A **559**, 190 (2006).
[17] R. A. Fisher, Ann. Eugenics **7**, 179 (1936).
[18] The Fox-Wolfram moments were introduced in G. C. Fox and S. Wolfram, Phys. Rev. Lett. **41**, 1581 (1978); The modified moments used in this Letter are described in S. H. Lee *et al.* (Belle Collaboration), Phys. Rev. Lett. **91**, 261801 (2003).
[19] H. Kakuno *et al.* (Belle Collaboration), Nucl. Instrum. Methods Phys. Res., Sect. A **533**, 516 (2004).
[20] B. Aubert *et al.* (BaBar Collaboration), Phys. Rev. Lett. **99**, 221801 (2007).